Supplement of Atmos. Chem. Phys., 25, 12569–12584, 2025
https://doi.org/10.5194/acp-25-12569-2025-supplement

Atmospheric Chemistry and Physics
Open Access

Supplement of

Rapid aqueous-phase oxidation of an α-pinene-derived organosulfate by hydroxyl radicals: a potential source of some unclassified oxygenated and small organosulfates in the atmosphere

Donger Lai et al.

Correspondence to: Yuchen Wang (ywang@hnu.edu.cn) and Man Nin Chan (mnchan@cuhk.edu.hk)

CONTENTS

Section S1. Summary of abundance of *α*pOS-249 reported in previous studies

Table S1. A summary of abundance of *α*pOS-249 in atmospheric aerosols reported in previous studies.

Sampling location	Sampling season	Average concentration of *α*pOS-249 (ng/m^3)	Average concentration of total OSs (ng/m^3)[a]	Mass ratio of *α*pOS-249 to total OSs	Average concentration of inorganic sulfate (μg/m^3)	References
Silkeborg, Denmark	Spring, 2008	0.04	0.37	10.8 %	Not reported	(Kristensen and Glasius, 2011)
Skagerrak, Norway	Summer, 2009	0.05	0.85	5.9 %	Not reported	(Yttri et al., 2011)
Helsinki, Finland	Summer, 2009	0.08	1.43	5.6 %	Not reported	(Yttri et al., 2011)
Guangdong, China	Winter, 2010	0.41	2.71	15.1 %	18.70	(Wang et al., 2017)
Hong Kong, China	Winter, 2010	0.08	0.88	9.1 %	9.70	(Wang et al., 2017)
Shanghai, China	Spring, 2012	0.09	0.51	17.7 %	Not reported	(Ma et al., 2014)
Shanghai, China	Summer, 2012	0.37	26.69	1.4 %	Not reported	(Ma et al., 2014)
Shanghai, China	Autumn, 2012	0.17	1.56	10.9 %	Not reported	(Ma et al., 2014)
Guangdong, China	Summer & Winter, 2012	0.06	0.82	7.3 %	Not reported	(Wang et al., 2019)
Shanghai, China	Winter, 2013	0.14	1.13	12.4 %	Not reported	(Ma et al., 2014)
Beijing, China	Summer, 2016	0.06	55.2	0.1 %	Not reported	(Wang et al., 2018)
Hong Kong, China	Autumn, 2016 Summer, 2017	0.05	0.37	13.5 %	Not reported	(Wang et al., 2019)
Shanghai, China	Spring, 2017	0.05	0.50	10.0 %	Not reported	(Wang et al., 2019)

[a]Total OSs represents the total quantified concentrations of organosulfates.

Section S2. Summary of experimental details

A series of experiments were conducted and summarized below (**Table S2**). The experiments encompassed kinetic experiments (*α*pOS-249 + reference compound (i.e., benzoic acid (BA)) + •OH), product-capture experiments (*α*pOS-249 + •OH), and control experiments (*α*pOS-249 + UV light only and *α*pOS-249 + H_2O_2 only). Duplicate experiments were performed for each condition.

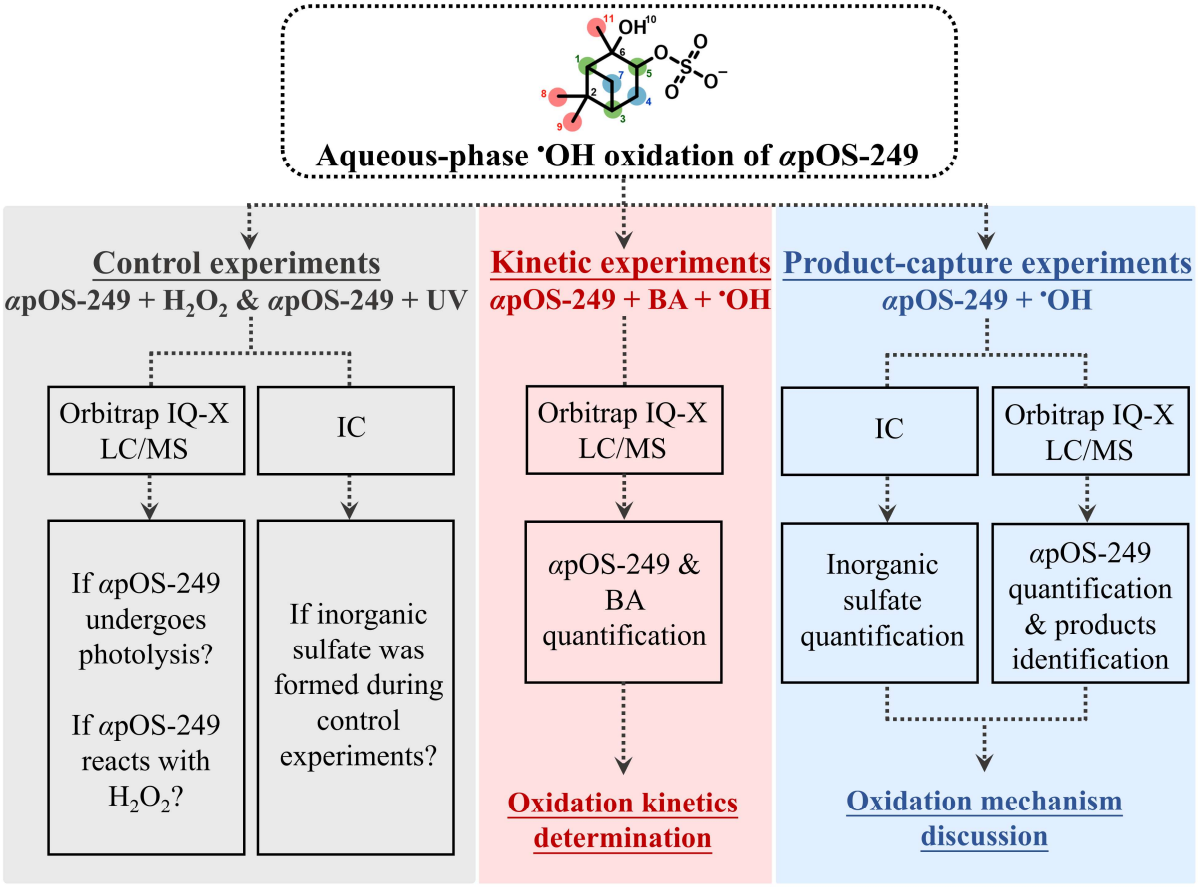

Scheme S1. An overview of the experimental design and chemical analysis in this work.

Table S2. A summary of experimental conditions used in the series of aqueous-phase experiments.

Reactants		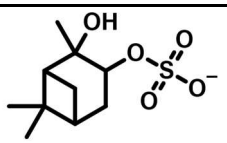 **α-pinene derived organosulfate (αpOS-249, $C_{10}H_{17}SO_5^-$)**			
Experimental Details		**Control experiments**		**Kinetic experiments**	**Product-capture experiments**
Reactions		**αpOS-249 + H_2O_2**	**αpOS-249 + UV**	**αpOS-249 + BA + $^{\bullet}$OH**	**αpOS-249 + $^{\bullet}$OH**
Concentrations (mol L^{-1})	**[αpOS-249]**	5×10^{-5}	5×10^{-5}	5×10^{-5}	5×10^{-5}
	[H_2O_2]	2×10^{-3}	–	2×10^{-3}	2×10^{-3}
	[BA]	–	–	5×10^{-5}	–
	[$^{\bullet}$OH]$_{ss}$[a]	–	–	6×10^{-14}	9×10^{-14}
Measured pH values	**Before oxidation**	5.4 ± 0.2	5.3 ± 0.3	4.5 ± 0.2	5.4 ± 0.2
	After oxidation	5.3 ± 0.3	5.2 ± 0.3	4.5 ± 0.1	4.3 ± 0.2

[a]Steady-state concentration of $^{\bullet}$OH ([$^{\bullet}$OH]$_{ss}$) was calculated from the simulations using the kinetic box model (**Section S3**).

Section S3. Evaluation of steady-state concentration of ˙OH ($[OH]_{ss}$)

Table S3. Reaction schemes and rate constants for the kinetic box model.

No.	Reactions	Parameters	References
R1	$H_2O_2 + h\nu$ (λ = 313 nm) → 2˙OH	Φ = 0.93	(Herrmann et al., 2010)
R2	2 × ˙OH → H_2O_2	5.5×10^9 M^{-1} s^{-1}	(Buxton et al., 1988)
R3	˙OH + H_2O_2 → HO_2˙ + H_2O	3.0×10^7 M^{-1} s^{-1}	(Christensen et al., 1982)
R4	˙OH + HO_2˙→ H_2O + O_2	1.0×10^{10} M^{-1} s^{-1}	(Elliot and Buxton, 1992)
R5	˙OH + O_2˙⁻→ OH^- + O_2	1.1×10^{10} M^{-1} s^{-1}	(Christensen et al., 1989)
R6	$H_2O \rightleftharpoons H^+ + OH^-$	pK_a = 13.999	(Pastina and Laverne, 2001)
R7	HO_2˙ ⇌ H^+ + O_2˙⁻	pK_a = 4.8	(Buxton et al., 1988)
R8	2 × HO_2˙ → H_2O_2 + O_2	9.8×10^5 M^{-1} s^{-1}	(Christensen et al., 1989)
R9	2 × O_2˙⁻ + 2 × H_2O → H_2O_2 + O_2 + 2 × OH^-	3.5×10^{-1} M^{-1} s^{-1}	(Judith and Bielski, 1979)
R10	HO_2˙ + H_2O_2 → ˙OH + O_2 + H_2O	5.0×10^{-1} M^{-1} s^{-1}	(Pastina and Laverne, 2001)
R11	O_2˙⁻ + H_2O_2 → ˙OH + O_2 + OH^-	1.3×10^{-1} M^{-1} s^{-1}	(Bielski et al., 1985)
R12	˙OH + *α*pOS-249 → Products	$(2.2 \pm 0.2) \times 10^9$ M^{-1} s^{-1}	This work
R13	˙OH + BA → Products	$(5.5 \pm 0.3) \times 10^9$ M^{-1} s^{-1}	This work[a]

[a]This reaction is included only in the kinetic study and not in the product study.

Section S4. Control experiments

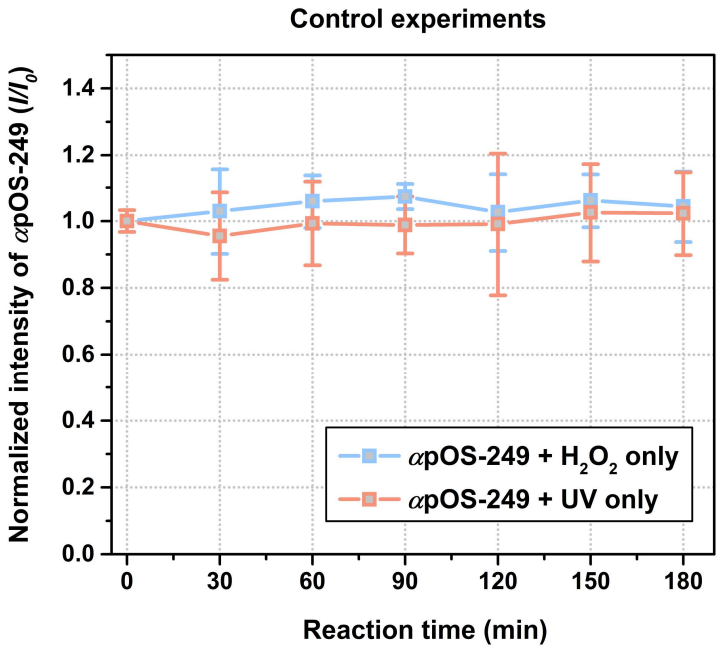

Figure S1. Normalized intensity analysis using Orbitrap IQ-X LC/MS in control experiments to examine the effects of H_2O_2 and UV light on αpOS-249.

Section S5. pH effects and the second-order rate constant of benzoic acid with •OH in the aqueous phase

We acknowledge that pH can be an important factor affecting the kinetics of aqueous-phase •OH oxidation. This phenomenon can be attributed to the pH-dependent speciation of organic compounds, which exist in different ionic forms (protonated, partially deprotonated, and deprotonated), depending on the solution acidity. These different states can alter the reaction mechanisms, potentially modifying electron transfer pathways or electronic effects, thereby influencing the overall oxidative kinetics (Chu et al., 2023). In our study, the dissociation constants (pK_{a1} = −3.5 and pK_{a2} = 12.2) of αpOS-249 (Pan et al., 2021) indicate that it predominantly exists in its singly deprotonated form across the pH range from −1 to 10. The reaction kinetics is likely not sensitive to the solution pH (Tilgner et al., 2021). Furthermore, a recent laboratory study has investigated the aqueous-phase •OH oxidation of five atmospherically relevant OSs (methyl sulfate, ethyl sulfate, propyl sulfate, hydroxyacetone sulfate and phenyl sulfate) as a function of pH (Gweme and Styler, 2024). It was reported that the rate constants were not sensitive to pH, remaining identical within experimental error under both acidic (pH = 2) and basic (pH = 9) conditions. This stability is attributed to the fact that all the investigated OSs existed exclusively in their anionic form in the aqueous phase at these pH levels (Gweme and Styler, 2024). Taken together, the cumulative evidence suggests that the reaction kinetics of aqueous-phase •OH oxidation of αpOS-249 are likely not sensitive to the pH under typical atmospheric conditions.

Previous study determined the second-order rate constant for the reaction of benzoic acid with •OH in aqueous phase to be $k = 4.3 \times 10^9$ L mol^{-1} s^{-1} for the undissociated form (HA, C_6H_5COOH) and $k = 6.0 \times 10^9$ L mol^{-1} s^{-1} for the deprotonated form (A^-, $C_6H_5COO^-$) (Simic and Hoffman, 1972; Ayatollahi et al., 2013). In our study, with a solution pH of 4.5 and using an average dissociation constant $pK_a = 4.14$ (Jover et al., 2008), we calculated the second-order rate constant for benzoic acid at this pH to be $(5.5 \pm 0.3) \times 10^9$ L mol^{-1} s^{-1} (Schaefer et al., 2020).

Section S6. Structure-Activity Relationship (SAR) model

Table S4. The H-abstraction rate for different reaction sites of *α*pOS-249 predicted by the SAR model. In the molecular structure, red, blue, and green markings represent primary, secondary, and tertiary carbon atoms, respectively.

Chemical structure	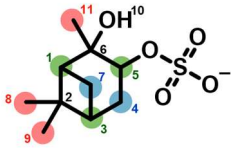 **α-pinene-derived organosulfate ($C_{10}H_{17}O_5SNa$, αpOS-249)**			
	Reaction sites	**Reaction rates (L mol^{-1} s^{-1})[a]**	**Partial rate constant/ Total rate constant (%)**	
Primary carbon	**8-C** **9-C** **11-C**	4.51×10^8 4.51×10^8 1.70×10^8	14.65 14.65 5.51	34.81[b]
Secondary carbon	**4-C** **7-C**	3.88×10^8 5.29×10^8	12.58 17.15	29.73[b]
Tertiary carbon	**1-C** **3-C** **5-C**	2.78×10^8 6.54×10^8 0.71×10^8	9.03 21.23 2.30	32.57[b]
Hydroxyl group (−OH)	**10−OH**	0.89×10^8	2.89	2.89[b]
Total		$\mathbf{3.08 \times 10^9}$	**100**	**100**

[a]Prediction made by using the dataset developed by Monod and Doussin (2008) and new parameters from our previous work with $F(-OSO_3^-) = 0.22$ and $G(-OSO_3^-) = 0.44$ (Lai et al., 2024). [b]The values represent total partial rate constant (considering carbon atoms such as primary, secondary, and tertiary carbons) divided by total rate constant (%).

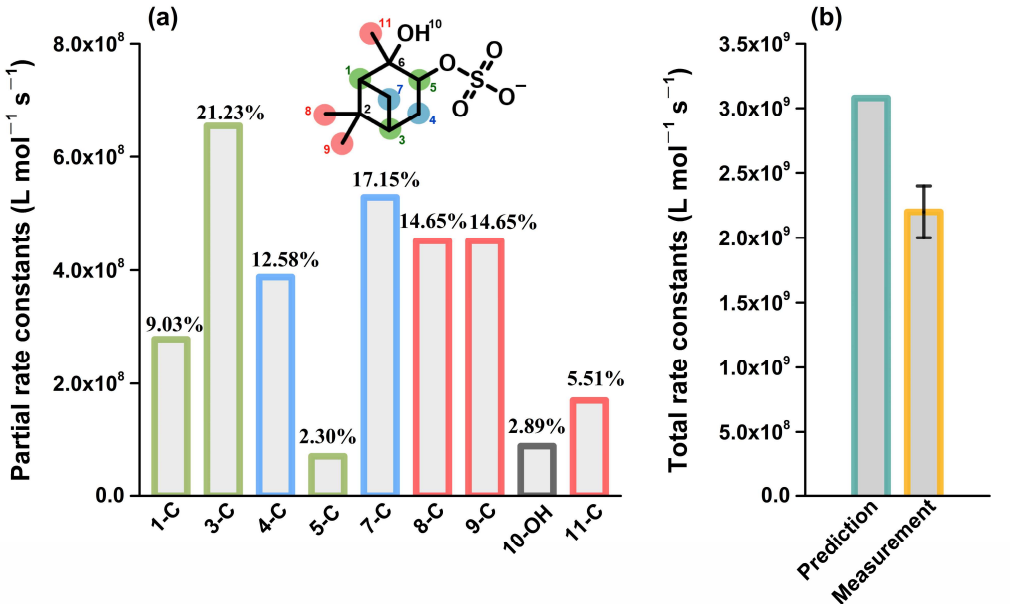

Figure S2. Calculated partial rate constants of H-abstraction from different positions based on SAR model and experimental results of the *α*pOS-249 aqueous-phase ·OH oxidation. Percentages above each column represent relative reactivity.

Section S7. Summary of detected OS products upon the aqueous •OH oxidation of *α*pOS-249

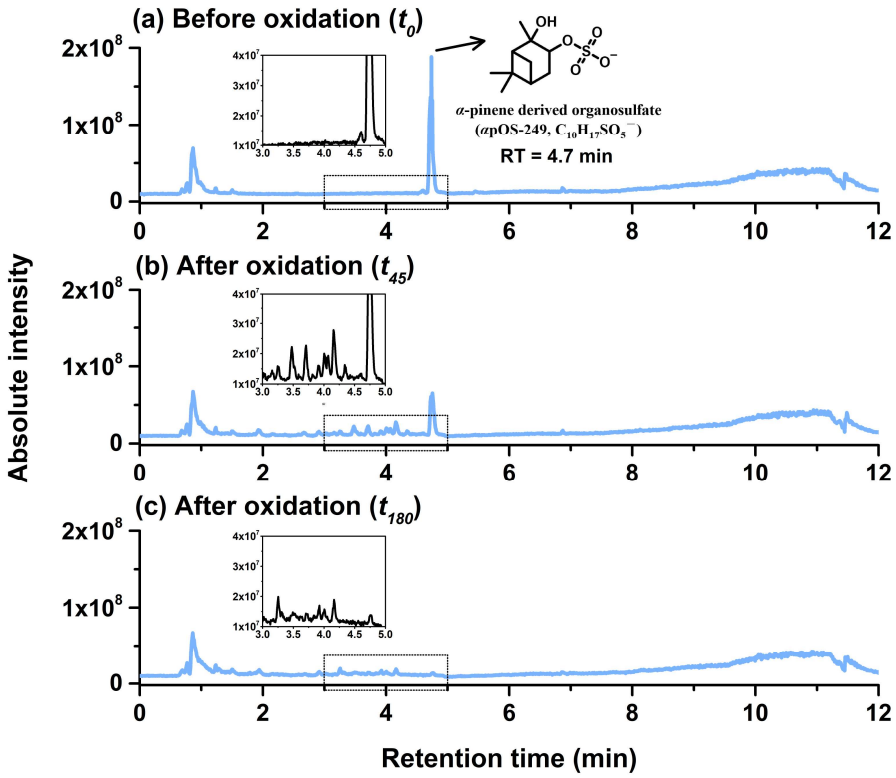

Figure S3. Total ion chromatograms (TIC) obtained with Orbitrap IQ-X LC/MS: (a) at t_0 (before oxidation), and (b) at t_{45} and (c) at t_{180} (after the aqueous-phase •OH oxidation of *α*pOS-249). The black line depicted in the figure represents an enlarged TIC specifically captured at a retention time of 3 to 5 min.

Table S5. Summary of detected OS upon the aqueous ·OH oxidation of *α*pOS-249 (product study of "*α*pOS-249 + ·OH").

OSs				Previous studies					This work	
Formula	**Theoretical *m*/*z***	**Detected *m*/*z*[a]**	**Retention time (min)**	**Detected in the ambient samples**	**Atmospheric abundance (ng/m^3)**	**Suggested precursor**	**Suggested formation pathway**	**Ref.**	**Additional formation pathway**	**Suggested new formation pathway**
Smaller OS (<C$_{10}$) products										
$C_3H_5SO_5^-$	152.9858	152.9855	0.94; 1.13	Yes	0.31−17.30	Isoprene/glycolaldehyde/ hydroxyacetone	Isoprene + ·OH + (NO) + acidic/neutral sulfate seed	(Surratt et al., 2008; Ma et al., 2014; Hansen et al., 2014; Nguyen et al., 2014; Hettiyadura et al., 2015; Meade et al., 2016; Kristensen et al., 2016; Hettiyadura et al., 2017; Glasius et al., 2018; Huang et al., 2018; Wang et al., 2018; Hughes and Stone, 2019; Hettiyadura et al., 2019; Wang et al., 2023)	✓	
$C_5H_7SO_7^-$	210.9913	210.9912	1.05; 1.28	Yes	0.17−131.00	Isoprene	Isoprene + ·OH + acidic sulfate seed	(Surratt et al., 2008; Nguyen et al., 2014; Kristensen et al., 2016; Rattanavaraha et al., 2017; Wang et al., 2018; Glasius et al., 2018; Le Breton et al., 2018; Hughes and Stone, 2019; Hettiyadura et al., 2019)	✓	
$C_6H_9SO_6^-$	209.0120	209.0116	1.24; 1.35; 1.78	Yes	10.20	Anthropogenic	**Unknown**	(Hettiyadura et al., 2019; Hughes and Stone, 2019)		✓
$C_6H_7SO_7^-$	222.9913	222.9911	0.94; 1.12; 1.23; 1.38; 3.92	Yes	Not reported	**Unknown**	**Unknown**	(Kuang et al., 2016)		✓
$C_6H_7SO_8^-$	238.9862	238.9859	1.05; 1.23; 1.56; 1.74	No	–	–	–	–		
$C_6H_9SO_8^-$	241.0018	241.0014	0.91; 1.12	Yes	Not reported	**Unknown**	**Unknown**	(Kuang et al., 2016)		✓
$C_7H_7SO_7^-$	234.9913	234.9910	1.36	No	–	–	–	–		

$C_7H_9SO_7^-$	237.0069	237.0065	0.95; 1.12; 1.32; 1.58; 2.01; 2.27; 2.63; 3.01; 3.51	Yes	0.01−6.60	Isoprene	Methyl vinyl ketone + $SO_4^{\bullet-}$	(Nozière et al., 2010; Hettiyadura et al., 2019)	✓	
$C_7H_9SO_8^-$	253.0018	253.0017	0.93; 1.07; 1.78; 2.96; 3.93	Yes	Not reported	**Unknown**	**Unknown**	(Mutzel et al., 2015; Brüggemann et al., 2017)		✓
$C_7H_{11}SO_8^-$	255.0175	255.0168	0.94; 1.23; 1.49	Yes	Not reported	**Unknown**	**Unknown**	(Kuang et al., 2016)		✓
$C_7H_7SO_9^-$	266.9811	266.9808	1.04	No	–	–	–	–		
$C_7H_9SO_9^-$	268.9967	268.9960	0.94; 1.22	No	–	–	–	–		
$C_7H_{11}SO_9^-$	271.0124	271.0120	0.92; 1.09; 1.21	Yes	0.13−0.24	**Unknown**	**Unknown**	(Yang et al., 2023)		✓
$C_7H_{11}SO_{10}^-$	287.0073	287.0066	0.94	Yes	0.15−0.23	**Unknown**	**Unknown**	(Yang et al., 2023)		✓
$C_8H_9SO_6^-$	233.0120	233.0117	3.32	Yes	Not reported	**Unknown**	**Unknown**	(Kuang et al., 2016)		✓
$C_8H_{11}SO_7^-$	251.0226	251.0221	1.35; 1.64; 1.97; 2.30; 2.73; 3.01; 3.31; 3.49	Yes	Not reported	Isoprene	Methyl vinyl ketone/methacrolein + $SO_4^{\bullet-}$	(Nozière et al., 2010; Schindelka et al., 2013; Kuang et al., 2016)	✓	
$C_8H_{11}SO_8^-$	267.0175	267.0169	1.10; 1.30; 1.55; 1.77; 1.94; 2.25; 2.62	Yes	0.02	**Unknown**	**Unknown**	(Meade et al., 2016)		✓
$C_8H_{11}SO_9^-$	283.0124	283.0116	1.04; 1.35; 1.70; 2.05	Yes	Not reported	**Unknown**	**Unknown**	(Kuang et al., 2016)		✓
$C_9H_{15}SO_5^-$	235.0640	235.0635	4.21; 4.52; 4.66	Yes	0.13−1.62	Monoterpenes	**Unknown**	(Meade et al., 2016; Brüggemann et al., 2019)		✓
$C_9H_{13}SO_6^-$	249.0433	249.0427	1.72; 2.32; 2.82; 3.03; 3.19; 3.52; 3.74; 4.04; 4.39; 4.76	Yes	0.22	Monoterpenes	Limonene/terpinolene + $^{\bullet}OH$ + NO + highly acidic sulfate seed	(Surratt et al., 2008; Brüggemann et al., 2019)	✓	
$C_9H_{15}SO_6^-$	251.0589	251.0585	1.23; 2.07; 2.21; 3.28; 3.54; 3.79; 3.96	Yes	0.06−8.00	Monoterpenes/sesquiterpenes	limonene + $^{\bullet}OH$ + (NO) + (highly) acidic sulfate seed	(Surratt et al., 2008; Nguyen et al., 2014; Kristensen et al., 2016; Wang et al., 2018; Hettiyadura et al., 2019; Brüggemann et al., 2019; Hughes and Stone, 2019)	✓	

$C_9H_{11}SO_7^-$	263.0226	263.0211	1.67; 2.20; 2.61; 2.77; 3.48; 3.70; 4.01	Yes	0.05−0.13	Monoterpenes	**Unknown**	(Yttri et al., 2011; Brüggemann et al., 2019)		✓
$C_9H_{13}SO_7^-$	265.0382	265.0376	1.22; 1.93; 2.15; 3.22; 3.50; 3.64; 3.98; 4.21	Yes	0.68−1.57	Monoterpenes	**Unknown**	(Brüggemann et al., 2019)		✓
$C_9H_{15}SO_7^-$	267.0539	267.0532	1.41; 1.55; 2.14; 2.43; 2.97; 3.50	Yes	0.26−8.13	Isoprene/monoterpenes/ anthropogenic	limonene + $^{\bullet}OH$ + NO + highly acidic sulfate seed	(Surratt et al., 2008; Nguyen et al., 2014; Riva et al., 2016; Meade et al., 2016; Brüggemann et al., 2019; Hughes and Stone, 2019)	✓	
$C_9H_{13}SO_8^-$	281.0331	281.0325	1.24; 1.50; 1.68; 1.86; 1.97; 2.37; 2.57; 3.24; 3.73	Yes	1.79−1.93	Monoterpenes	**Unknown**	(Brüggemann et al., 2019)		✓
$C_9H_{15}SO_8^-$	283.0488	283.0479	1.12; 1.23; 1.38; 1.57; 1.75; 1.93; 2.13; 2.24; 3.34; 3.88	Yes	0.16−1.30	Monoterpenes	α-terpinene + $^{\bullet}OH$ + NO + highly acidic sulfate seed	(Surratt et al., 2008; Meade et al., 2016; Brüggemann et al., 2019)	✓	
More oxygenated C_{10} OS products										
$C_{10}H_{15}SO_5^-$	247.0640	247.0636	4.47; 4.58	Yes	0.02−0.80	Monoterpenes	α-pinene + $^{\bullet}OH/NO_3^{\bullet}$ + highly acidic sulfate seed	(Surratt et al., 2008; Nguyen et al., 2014; Ma et al., 2014; Brüggemann et al., 2019)	✓	
$C_{10}H_{15}SO_6^-$	263.0589	263.0584	3.47; 3.69; 3.82; 4.16; 4.34; 4.82	Yes	0.11	Monoterpenes	β-pinene + $^{\bullet}OH$ + NO + highly acidic sulfate seed	(Surratt et al., 2008; Ma et al., 2014)	✓	
$C_{10}H_{17}SO_6^-$	265.0746	265.0741	1.92; 1.97; 3.13; 3.41; 4.04; 4.15; 4.43	Yes	0.08−3.58	Monoterpenes/anthropogenic	α-pinene/α-terpinene/terpinolene + $^{\bullet}OH$ + (NO) + (highly) acidic sulfate seed	(Surratt et al., 2008; Ma et al., 2014; Riva et al., 2016; Brüggemann et al., 2019)	✓	
$C_{10}H_{13}SO_7^-$	277.0382	277.0377	2.53; 2.74; 2.82; 2.97; 3.34; 3.66; 3.73; 3.97; 4.25; 4.36; 4.59	Yes	Not reported	**Unknown**	**Unknown**	(Kuang et al., 2016)		✓

$C_{10}H_{15}SO_7^-$	279.0539	279.0532	1.85; 2.37; 2.51; 2.76; 3.24; 3.37; 3.58; 3.70; 4.00	Yes	0.03−7.10	Monoterpenes/anthropogenic	*α*-pinene/*β*-pinene/limonene/*α*-terpinene/*γ*-terpinene + $^{\bullet}OH/NO_3^{\bullet}/SO_4^{\bullet-}$ + (NO) + (highly) acidic sulfate seed	(Surratt et al., 2008; Nozière et al., 2010; Kristensen and Glasius, 2011; Yttri et al., 2011; Ma et al., 2014; Nguyen et al., 2014; Meade et al., 2016; Riva et al., 2016; Hettiyadura et al., 2019; Brüggemann et al., 2019; Hughes and Stone, 2019)	✓	
$C_{10}H_{17}SO_7^-$	281.0695	281.0689	2.63; 2.90; 3.10; 3.61	Yes	0.16−12.10	Monoterpenes	*α*-pinene/*β*-pinene /limonene/*α*-terpinene/terpinolene + $^{\bullet}OH/SO_4^{\bullet-}$ + (NO) + (highly) acidic sulfate seed	(Surratt et al., 2008; Nozière et al., 2010; Ma et al., 2014; Hettiyadura et al., 2019; Hughes and Stone, 2019)	✓	
$C_{10}H_{13}SO_8^-$	293.0331	293.0323	1.56; 1.75; 1.89; 2.05; 2.23; 3.04; 3.31; 3.44; 3.73; 3.87; 4.30	Yes	Not reported	**Unknown**	**Unknown**	(Kuang et al., 2016)		✓
$C_{10}H_{15}SO_8^-$	295.0488	295.0480	1.22; 1.42; 1.57; 1.77; 1.87; 2.11; 2.54; 3.31; 3.51; 3.83; 4.36	Yes	0.28−1.53	Monoterpenes/anthropogenic	**Unknown**	(Riva et al., 2016; Brüggemann et al., 2019)		✓
$C_{10}H_{17}SO_8^-$	297.0644	297.0641	1.43; 1.73; 2.04; 2.26; 3.02; 3.43	Yes	0.05−1.55	Monoterpenes/anthropogenic	*α*-pinene/*α*-terpinene/terpinolene + $^{\bullet}OH/SO_4^{\bullet-}$ + (NO) + (highly) acidic sulfate seed	(Surratt et al., 2008; Nozière et al., 2010; Nguyen et al., 2014; Riva et al., 2016; Meade et al., 2016; Brüggemann et al., 2019)	✓	
$C_{10}H_{13}SO_9^-$	309.0280	309.0275	1.23; 1.47; 1.70; 2.16; 2.55; 3.26; 3.50; 3.85; 4.74	Yes	0.30−0.54	Monoterpenes	**Unknown**	(Brüggemann et al., 2019)		✓
$C_{10}H_{15}SO_9^-$	311.0437	311.0428	1.23; 1.44; 1.77; 3.24; 3.65; 3.91; 4.12	Yes	Not reported	**Unknown**	**Unknown**	(Kuang et al., 2016)		✓

$C_{10}H_{13}SO_{10}^-$	325.0229	325.0221	1.22; 1.43; 1.58; 1.86; 2.49	No	–	–		–		
$C_{10}H_{15}SO_{10}^-$	327.0386	327.0374	1.22; 1.43; 1.60; 1.78; 1.83; 3.30	Yes	Not reported	**Unknown**	**Unknown**	(Kuang et al., 2016)		✓
$C_{10}H_{15}SO_{11}^-$	343.0335	343.0324	1.06; 1.23; 1.34; 1.52; 1.61; 3.41	No	–	–		–		

[a]Data were collected using Orbitrap IQ-X LC/MS with mass tolerance of ±5 ppm to their theoretical masses.

Section S8. Evolutions in absolute intensity of the composition with different carbon atoms

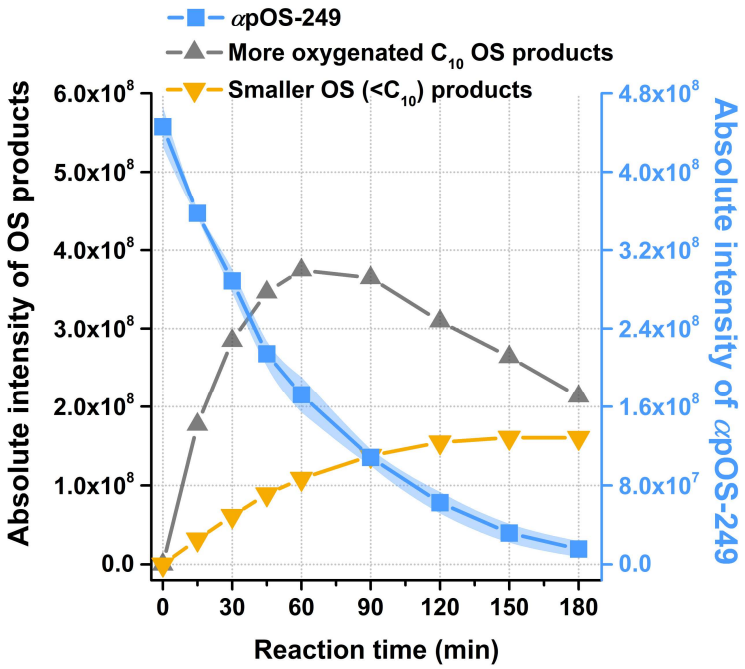

Figure S4. Time-dependent evolution of absolute intensities for αpOS-249 decay and reaction products formed during the aqueous-phase ·OH oxidation of αpOS-249.

Section S9. Reaction mechanisms

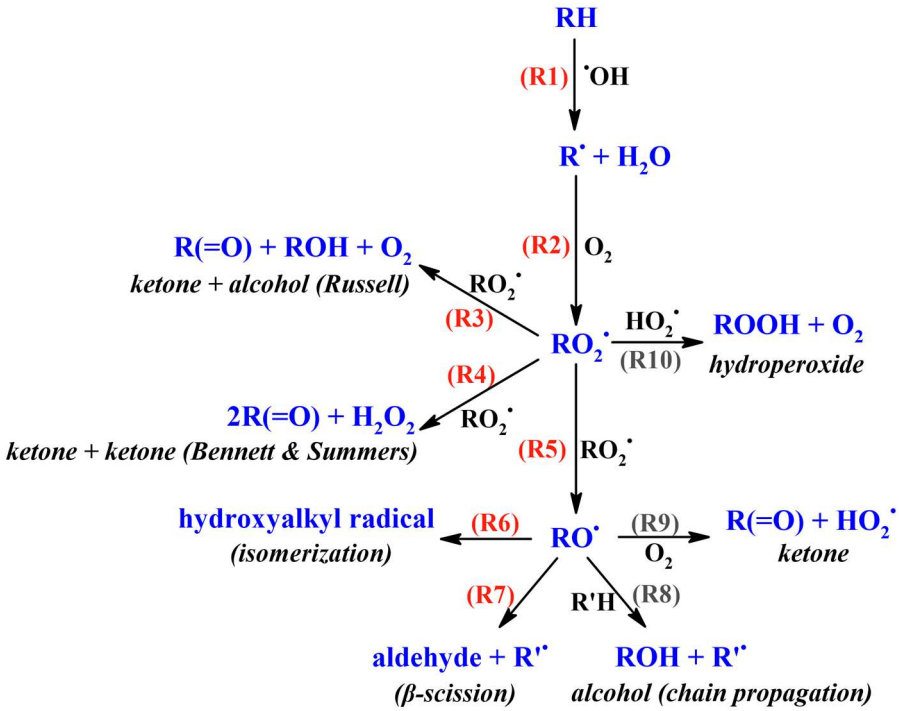

Scheme S2. A generic reaction mechanism for the aqueous-phase ·OH oxidation of *α*pOS-249.

These 40 identified OS products, formed through the reaction of ·OH radicals in the presence of dissolved oxygen (O_2), can be interpreted within the framework of the established aqueous-phase oxidation mechanism, as shown in **Scheme S2** (Hearn et al., 2007; Smith et al., 2009). Before oxidation, *α*pOS-249 primarily exists in its anionic form. The oxidation process typically initiates with H-abstraction by ·OH radicals from organic compound (RH), leading to the formation of an alkyl radical (R·). These alkyl radicals then rapidly combine with O_2 to produce peroxyl radical (RO_2·). The initial reaction can occur at multiple sites on the *α*pOS-249 molecule, yielding a diverse array of first-generation products with different structural isomers. These possible first-generation products arises from several reaction pathways: i) generation of hydroperoxides (**Scheme S2, R10**) (Smith et al., 2009), ii) formation of intermediate alkoxy radicals (RO·) (**Scheme S2, R5**) (George and Abbatt, 2010; Kroll et al., 2015), iii) production of alcohol and carbonyl compounds via Russell reactions (**Scheme S2, R3**) (Russell, 1957), iv) formation of two carbonyl products through the Bennett and Summers mechanism (**Scheme S2, R4**) (Bennett and Summers, 1974). Moreover, multiple reaction pathways enable alkoxy radicals to produce both stable and radical intermediate products, resulting in the formation of lower-volatility oxygenated compounds in condensed phase. These possible pathways include: isomerization (**Scheme S2, R6**), chain propagation with

secondary RH loss (**Scheme S2, R8**), and O_2 reaction (**Scheme S2, R9**). The C-C bond β-scission decomposition of RO$^{\bullet}$ stands as the only known mechanism that generates higher-volatility, lower-molecular-weight products, forming an alkyl radical and aldehyde (**Scheme S2, R7**) (George and Abbatt, 2010). Overall, as the oxidation progresses, the first-generation products can further react with $^{\bullet}$OH radicals, forming second-generation and multi-generation products with their own set of isomers. This complexity makes it challenging to propose a comprehensive mechanism. Given this intricacy, only a generic reaction scheme is depicted for simplicity and clarity.

Section S10. Formation of inorganic sulfates and non-sulfated products

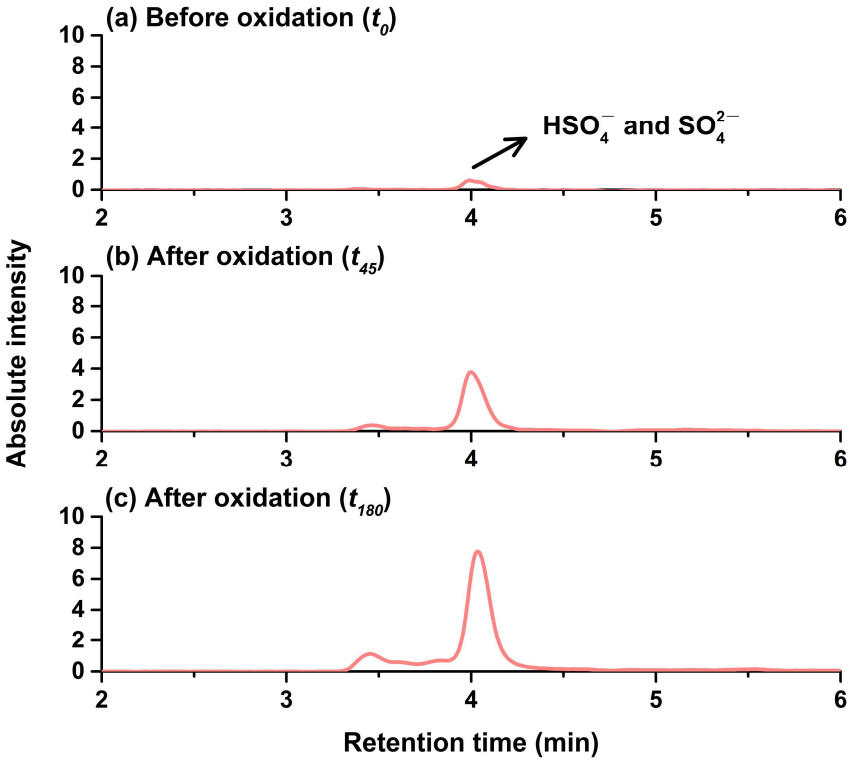

Figure S5. Ion chromatograms before (t_0) and after (t_{45} and t_{180}) the aqueous-phase $^{\bullet}$OH oxidation of *α*pOS-249.

Inorganic sulfates yield during the aqueous-phase $^{\bullet}$OH oxidation of *α*pOS-249

The formation of inorganic sulfates was quantified to determine the extent of total sulfur conversion, defined as the number of moles of inorganic sulfates formed per mole of *α*pOS-249 reacted as function of reaction time:

$$\text{Yield} = \frac{\Delta\left[SO_4^{2-}\right]}{\Delta\left[\alpha\text{pOS-249}\right]} \times 100\ \%$$

Where the concentration of inorganic sulfates was measured by IC, and the concentration of *α*pOS-249 was quantified by LC-ESI-Orbitrap MS.

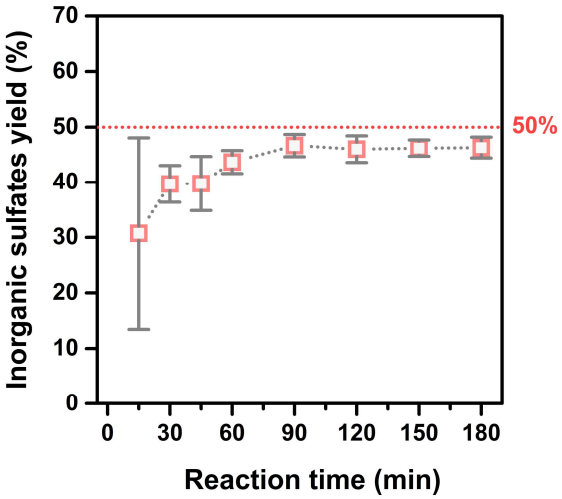

171

172 **Figure S6.** Inorganic sulfates (HSO_4^- and SO_4^{2-}) yield as function of reaction time during the

173 aqueous-phase ·OH oxidation of *α*pOS-249.

174

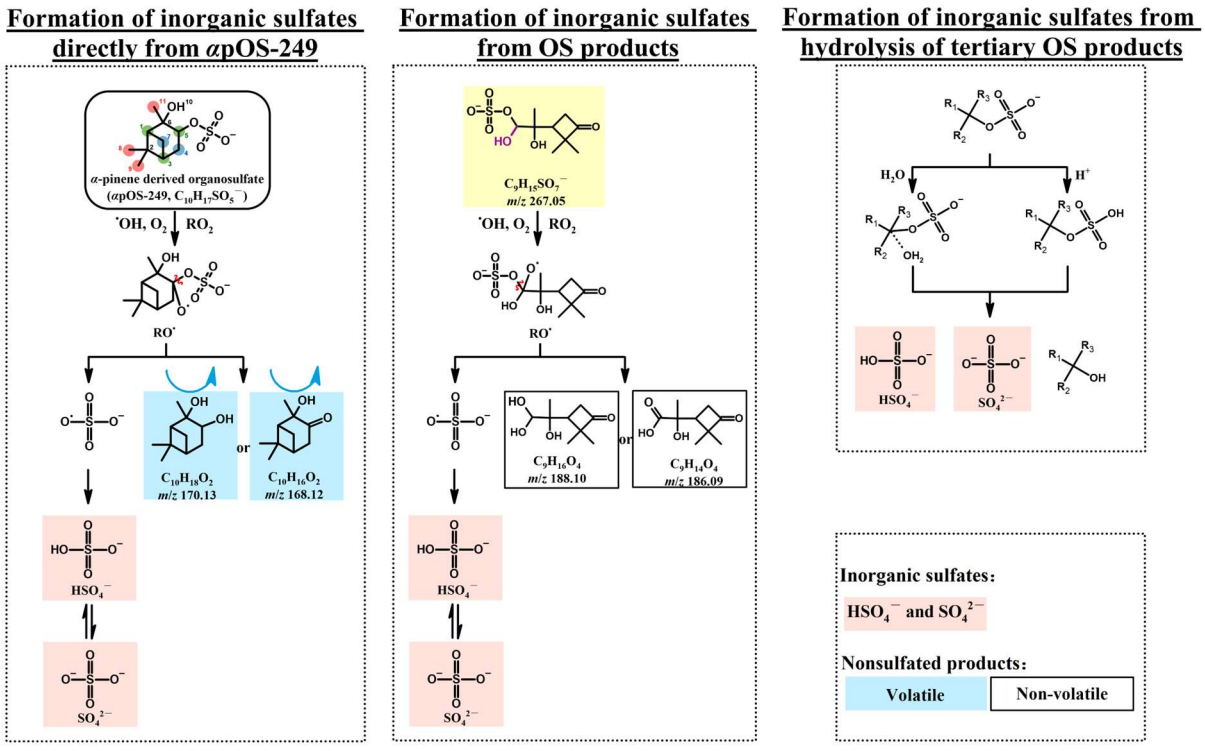

175

176 **Scheme S3.** Proposed mechanisms for the formation of inorganic sulfates and nonsulfated

177 products during the aqueous-phase ·OH oxidation of *α*pOS-249.

Section S11. Atmospheric implications

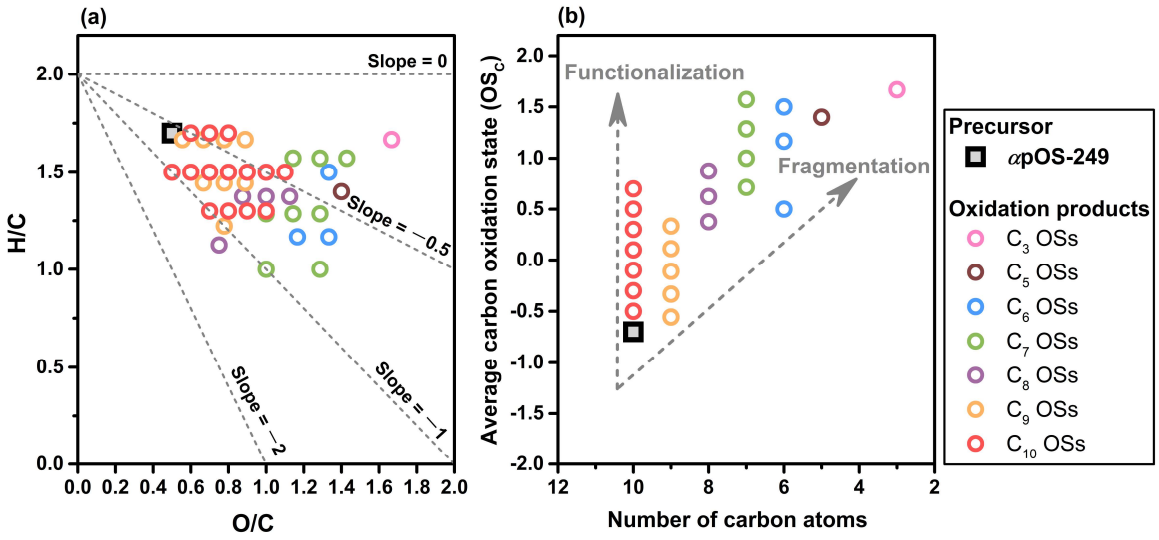

Figure S7. The evolution of composition of reaction products during the aqueous-phase •OH oxidation of *α*pOS-249 depicted in (a) the Van Krevelen diagram, and (b) the oxidation degree diagram.

Figure S7 shows the evolution of oxidation products during the aqueous-phase •OH oxidation of *α*pOS-249. The Van Krevelen diagram shows the spreading from C_{10} precursor of *α*pOS-249 towards to lower right (**Figure S7 (a)**), evolving into more oxygenated C_{10} OS products and smaller OS products with the O/C ratio increases and the H/C ratio decreases. Additionally, **Figure S7 (b)** demonstrates that oxidation involves both functionalization and fragmentation, with both processes contribute to the overall transformation of sulfur species.

References

Ayatollahi, S., Kalnina, D., Song, W., Turks, M., and Cooper, W. J.: Radiation chemistry of salicylic and methyl substituted salicylic acids: models for the radiation chemistry of pharmaceutical compounds, Radiat. Phys. Chem., 92, 93-98, https://doi.org/10.1016/j.radphyschem.2013.06.007, 2013.

Bennett, J. E. and Summers, R.: Product studies of the mutual termination reactions of sec-alkylperoxy radicals: Evidence for non-cyclic termination, Can. J. Chem., 52, 1377-1379, https://doi.org/10.1139/v74-209, 1974.

Bielski, B. H., Cabelli, D. E., Arudi, R. L., and Ross, A. B.: Reactivity of HO_2/O_2^- radicals in aqueous solution, J. Phys. Chem. Ref. Data., 14, 1041-1100, https://doi.org/10.1063/1.555739, 1985.

Brüggemann, M., Van Pinxteren, D., Wang, Y., Yu, J. Z., and Herrmann, H.: Quantification of known and unknown terpenoid organosulfates in PM_{10} using untargeted LC–HRMS/MS: contrasting summertime rural Germany and the North China Plain, Environ. Chem., 16, 333-346, https://doi.org/10.1071/EN19089, 2019.

Brüggemann, M., Poulain, L., Held, A., Stelzer, T., Zuth, C., Richters, S., Mutzel, A., van Pinxteren, D., Iinuma, Y., and Katkevica, S.: Real-time detection of highly oxidized organosulfates and BSOA marker compounds during the F-BEACh 2014 field study, Atmos. Chem. Phys., 17, 1453-1469, https://doi.org/10.5194/acp-17-1453-2017, 2017.

Buxton, G. V., Greenstock, C. L., Helman, W. P., and Ross, A. B.: Critical review of rate constants for reactions of hydrated electrons, hydrogen atoms and hydroxyl radicals ($\cdot OH/\cdot O^-$ in aqueous solution, J. Phys. Chem. Ref. Data., 17, 513-886, https://doi.org/10.1063/1.555805, 1988.

Christensen, H., Sehested, K., and Bjergbakke, E.: Radiolysis of reactor water: reaction of OH radicals with O_2^-, in: Water Chemistry of Nuclear Reactor Systems 5., 141-144, https://doi.org/10.1680/wconrs5v1.15470.0021, 1989.

Christensen, H., Sehested, K., and Corfitzen, H.: Reactions of hydroxyl radicals with hydrogen peroxide at ambient and elevated temperatures, J. Phys. Chem., 86, 1588-1590, https://doi.org/10.1021/j100206a023, 1982.

Chu, C., Yan, Y., Ma, J., Jin, S., Spinney, R., Dionysiou, D. D., Zhang, H., and Xiao, R.: Implementation of laser flash photolysis for radical-induced reactions and environmental implications, Water Res., 244, 120526, https://doi.org/10.1016/j.watres.2023.120526, 2023.

Elliot, A. J. and Buxton, G. V.: Temperature dependence of the reactions OH + O_2^- and OH + HO_2 in water up to 200 °C, J. Chem. Soc. Faraday Trans., 88, 2465-2470, 1992.

George, I. J. and Abbatt, J. P.: Heterogeneous oxidation of atmospheric aerosol particles by gas-phase radicals, Nat. Chem., 2, 713-722, https://doi.org/10.1038/nchem.806, 2010.

Glasius, M., Bering, M. S., Yee, L. D., de Sá, S. S., Isaacman-VanWertz, G., Wernis, R. A., Barbosa, H. M., Alexander, M. L., Palm, B. B., and Hu, W.: Organosulfates in aerosols downwind of an urban region in central Amazon, Environ. Sci. Process. Impacts., 20, 1546-1558, https://doi.org/10.1039/c8em00413g, 2018.

Gweme, D. T. and Styler, S. A.: OH Radical Oxidation of Organosulfates in the Atmospheric Aqueous Phase, J. Phys. Chem. A., 128, 9462-9475, https://doi.org/10.1021/acs.jpca.4c02877, 2024.

Hansen, A. M. K., Kristensen, K., Nguyen, Q., Zare, A., Cozzi, F., Nøjgaard, J. K., Skov, H., Brandt, J., Christensen, J. H., and Ström, J.: Organosulfates and organic acids in Arctic aerosols: speciation, annual variation and concentration levels, Atmos. Chem. Phys., 14, 7807-7823, https://doi.org/10.5194/acp-14-7807-2014, 2014.

Hearn, J. D., Renbaum, L. H., Wang, X., and Smith, G. D.: Kinetics and products from reaction of Cl radicals with dioctyl sebacate (DOS) particles in O_2: a model for radical-initiated oxidation of organic aerosols, Phys. Chem. Chem. Phys., 9, 4803-4813, https://doi.org/10.1039/b707523e, 2007.

Herrmann, H., Hoffmann, D., Schaefer, T., Brauer, P., and Tilgner, A.: Tropospheric aqueous-phase free-radical chemistry: radical sources, spectra, reaction kinetics and prediction tools, ChemPhysChem., 11, 3796-3822, https://doi.org/10.1002/cphc.201000533, 2010.

Hettiyadura, A., Stone, E., Kundu, S., Baker, Z., Geddes, E., Richards, K., and Humphry, T.: Determination of atmospheric organosulfates using HILIC chromatography with MS detection, Atmos. Meas. Tech., 8, 2347-2358, https://doi.org/10.5194/amt-8-2347-2015, 2015.

Hettiyadura, A. P., Jayarathne, T., Baumann, K., Goldstein, A. H., de Gouw, J. A., Koss, A., Keutsch, F. N., Skog, K., and Stone, E. A.: Qualitative and quantitative analysis of atmospheric organosulfates in Centreville, Alabama, Atmos. Chem. Phys., 17, 1343-1359, https://doi.org/10.5194/acp-17-1343-2017, 2017.

Hettiyadura, A. P. S., Al-Naiema, I. M., Hughes, D. D., Fang, T., and Stone, E. A.: Organosulfates in Atlanta, Georgia: anthropogenic influences on biogenic secondary organic aerosol formation, Atmos. Chem. Phys., 19, 3191-3206, https://doi.org/10.5194/acp-19-3191-2019, 2019.

Huang, R. J., Cao, J. J., Chen, Y., Yang, L., Shen, J. C., You, Q. H., Wang, K., Lin, C. S., Xu, W., Gao, B., Li, Y. J., Chen, Q., Hoffmann, T., O'Dowd, C. D., Bilde, M., and Glasius, M.: Organosulfates in atmospheric aerosol: synthesis and quantitative analysis of PM from Xi'an, northwestern China, Atmos. Meas. Tech., 11, 3447-3456, https://doi.org/10.5194/amt-11-3447-2018, 2018.

Hughes, D. D. and Stone, E. A.: Organosulfates in the Midwestern United States: abundance, composition and stability, Environ. Chem., 16, 312-322, https://doi.org/10.1071/En18260, 2019.

Jover, J., Bosque, R., and Sales, J.: QSPR prediction of pKa for benzoic acids in different solvents, QSAR Comb. Sci., 27, 563-581, https://doi.org/10.1002/qsar.200710095, 2008.

Judith, W. and Bielski, B.: Kinetics of the interaction of HO_2 and O_2^- radicals with hydrogen peroxide, J. Am. Chem. Soc., 101, 58-62, 1979.

Kristensen, K. and Glasius, M.: Organosulfates and oxidation products from biogenic hydrocarbons in fine aerosols from a forest in North West Europe during spring, Atmos. Environ., 45, 4546-4556, https://doi.org/10.1016/j.atmosenv.2011.05.063, 2011.

Kristensen, K., Bilde, M., Aalto, P. P., Petäjä, T., and Glasius, M.: Denuder/filter sampling of organic acids and organosulfates at urban and boreal forest sites: Gas/particle distribution and possible sampling artifacts, Atmos. Environ., 130, 36-53, https://doi.org/10.1016/j.atmosenv.2015.10.046, 2016.

Kroll, J. H., Lim, C. Y., Kessler, S. H., and Wilson, K. R.: Heterogeneous Oxidation of Atmospheric Organic Aerosol: Kinetics of Changes to the Amount and Oxidation State of Particle-Phase Organic Carbon, J. Phys. Chem. A., 119, 10767-10783, https://doi.org/10.1021/acs.jpca.5b06946, 2015.

Kuang, B. Y., Lin, P., Hu, M., and Yu, J. Z.: Aerosol size distribution characteristics of organosulfates in the Pearl River Delta region, China, Atmos. Environ., 130, 23-35, https://doi.org/10.1016/j.atmosenv.2015.09.024, 2016.

Lai, D. E., Schaefer, T., Zhang, Y. M., Li, Y. J., Xing, S. N., Herrmann, H., and Chan, M. N.: Deactivating Effect of Hydroxyl Radicals Reactivity by Sulfate and Sulfite Functional Groups in Aqueous Phase ─ Atmospheric Implications for Small Organosulfur Compounds, ACS ES&T Air., 1, 7, 678–689, https://doi.org/10.1021/acsestair.4c00033, 2024.

Le Breton, M., Wang, Y., Hallquist, Å. M., Pathak, R. K., Zheng, J., Yang, Y., Shang, D., Glasius, M., Bannan, T. J., and Liu, Q.: Online gas-and particle-phase measurements of organosulfates, organosulfonates and nitrooxy organosulfates in Beijing utilizing a FIGAERO

ToF-CIMS, Atmos. Chem. Phys., 18, 10355-10371, https://doi.org/10.5194/acp-18-10355-2018, 2018.

Ma, Y., Xu, X. K., Song, W. H., Geng, F. H., and Wang, L.: Seasonal and diurnal variations of particulate organosulfates in urban Shanghai, China, Atmos. Environ., 85, 152-160, https://doi.org/10.1016/j.atmosenv.2013.12.017, 2014.

Meade, L. E., Riva, M., Blomberg, M. Z., Brock, A. K., Qualters, E. M., Siejack, R. A., Ramakrishnan, K., Surratt, J. D., and Kautzman, K. E.: Seasonal variations of fine particulate organosulfates derived from biogenic and anthropogenic hydrocarbons in the mid-Atlantic United States, Atmos. Environ., 145, 405-414, https://doi.org/10.1016/j.atmosenv.2016.09.028, 2016.

Mutzel, A., Poulain, L., Berndt, T., Iinuma, Y., Rodigast, M., Boge, O., Richters, S., Spindler, G., Sipila, M., Jokinen, T., Kulmala, M., and Herrmann, H.: Highly Oxidized Multifunctional Organic Compounds Observed in Tropospheric Particles: A Field and Laboratory Study, Environ. Sci. Technol., 49, 7754-7761, https://doi.org/10.1021/acs.est.5b00885, 2015.

Nguyen, Q. T., Christensen, M. K., Cozzi, F., Zare, A., Hansen, A. M. K., Kristensen, K., Tulinius, T. E., Madsen, H. H., Christensen, J. H., Brandt, J., Massling, A., Nojgaard, J. K., and Glasius, M.: Understanding the anthropogenic influence on formation of biogenic secondary organic aerosols in Denmark via analysis of organosulfates and related oxidation products, Atmos. Chem. Phys., 14, 8961-8981, https://doi.org/10.5194/acp-14-8961-2014, 2014.

Nozière, B., Ekström, S., Alsberg, T., and Holmström, S.: Radical-initiated formation of organosulfates and surfactants in atmospheric aerosols, Geophys. Res. Lett., 37, https://doi.org/10.1029/2009GL041683, 2010.

Pan, X., Wang, H., Li, C., Zhang, J. Z., and Ji, C.: MolGpka: A web server for small molecule pKa prediction using a graph-convolutional neural network, J. Chem. Inf. Model., 61, 3159-3165, https://doi.org/10.1021/acs.jcim.1c00075, 2021.

Pastina, B. and LaVerne, J. A.: Effect of molecular hydrogen on hydrogen peroxide in water radiolysis, J. Phys. Chem. A., 105, 9316-9322, https://doi.org/10.1021/jp012245j, 2001.

Rattanavaraha, W., Chu, K., Budisulistiorini, S. H., Riva, M., Lin, Y. H., Edgerton, E. S., Baumann, K., Shaw, S. L., Guo, H., King, L., Weber, R. J., Neff, M. E., Stone, E. A., Offenberg, J. H., Zhang, Z., Gold, A., and Surratt, J. D.: Assessing the impact of anthropogenic pollution on isoprene-derived secondary organic aerosol formation in $PM_{2.5}$ collected from the

Birmingham, Alabama, ground site during the 2013 Southern Oxidant and Aerosol Study, Atmos. Chem. Phys., 16, 4897-4914, https://doi.org/10.5194/acp-16-4897-2016, 2017.

Riva, M., Barbosa, T. D., Lin, Y. H., Stone, E. A., Gold, A., and Surratt, J. D.: Chemical characterization of organosulfates in secondary organic aerosol derived from the photooxidation of alkanes, Atmos. Chem. Phys., 16, 11001-11018, https://doi.org/10.5194/acp-16-11001-2016, 2016.

Russell, G. A.: Deuterium-isotope effects in the autoxidation of aralkyl hydrocarbons. mechanism of the interaction of peroxy radicals[1], J. Am. Chem. Soc., 79, 3871-3877, https://doi.org/10.1021/ja01571a068, 1957.

Schaefer, T., Wen, L., Estelmann, A., Maak, J., and Herrmann, H.: pH- and Temperature-Dependent Kinetics of the Oxidation Reactions of OH with Succinic and Pimelic Acid in Aqueous Solution, Atmosphere., 11, 320, https://doi.org/10.3390/atmos11040320, 2020.

Schindelka, J., Iinuma, Y., Hoffmann, D., and Herrmann, H.: Sulfate radical-initiated formation of isoprene-derived organosulfates in atmospheric aerosols, Faraday. Discuss., 165, 237-259, https://doi.org/10.1039/c3fd00042g, 2013.

Simic, M. and Hoffman, M. Z.: Acid-base properties of the radicals produced in the pulse radiolysis of aqueous solutions of benzoic acid, J. Phys. Chem., 76, 1398-1404, https://doi.org/10.1021/j100654a004, 1972.

Smith, J., Kroll, J., Cappa, C., Che, D., Liu, C., Ahmed, M., Leone, S., Worsnop, D., and Wilson, K.: The heterogeneous reaction of hydroxyl radicals with sub-micron squalane particles: a model system for understanding the oxidative aging of ambient aerosols, Atmos. Chem. Phys., 9, 3209-3222, https://doi.org/10.5194/acp-9-3209-2009, 2009.

Surratt, J. D., Gomez-Gonzalez, Y., Chan, A. W., Vermeylen, R., Shahgholi, M., Kleindienst, T. E., Edney, E. O., Offenberg, J. H., Lewandowski, M., Jaoui, M., Maenhaut, W., Claeys, M., Flagan, R. C., and Seinfeld, J. H.: Organosulfate formation in biogenic secondary organic aerosol, J. Phys. Chem. A., 112, 8345-8378, https://doi.org/10.1021/jp802310p, 2008.

Tilgner, A., Schaefer, T., Alexander, B., Barth, M., Collett Jr, J. L., Fahey, K. M., Nenes, A., Pye, H. O., Herrmann, H., and McNeill, V. F.: Acidity and the multiphase chemistry of atmospheric aqueous particles and clouds, Atmos. Chem. Phys., 21, 13483-13536, https://doi.org/10.5194/acp-21-13483-2021, 2021.

Wang, Y., Ren, J., Huang, X. H. H., Tong, R., and Yu, J. Z.: Synthesis of Four Monoterpene-Derived Organosulfates and Their Quantification in Atmospheric Aerosol Samples, Environ. Sci. Technol., 51, 6791-6801, https://doi.org/10.1021/acs.est.7b01179, 2017.

354 Wang, Y., Ma, Y., Li, X., Kuang, B. Y., Huang, C., Tong, R., and Yu, J. Z.: Monoterpene and
355 sesquiterpene α-hydroxy organosulfates: synthesis, MS/MS characteristics, and ambient
356 presence, Environ. Sci. Technol., 53, 12278-12290, https://doi.org/10.1021/acs.est.9b04703,
357 2019.
358 Wang, Y., Hu, M., Guo, S., Wang, Y., Zheng, J., Yang, Y., Zhu, W., Tang, R., Li, X., and Liu,
359 Y.: The secondary formation of organosulfates under interactions between biogenic emissions
360 and anthropogenic pollutants in summer in Beijing, Atmos. Chem. Phys., 18, 10693-10713,
361 https://doi.org/10.5194/acp-18-10693-2018, 2018.
362 Wang, Y., Liang, S., Le Breton, M., Wang, Q. Q., Liu, Q., Ho, C. H., Kuang, B. Y., Wu, C.,
363 Hallquist, M., Tong, R., and Yu, J. Z.: Field observations of C2 and C3 organosulfates and
364 insights into their formation mechanisms at a suburban site in Hong Kong, Sci. Total. Environ.,
365 904, 166851, https://doi.org/10.1016/j.scitotenv.2023.166851, 2023.
366 Yang, T., Xu, Y., Ye, Q., Ma, Y. J., Wang, Y. C., Yu, J. Z., Duan, Y. S., Li, C. X., Xiao, H.
367 W., Li, Z. Y., Zhao, Y., and Xiao, H. Y.: Spatial and diurnal variations of aerosol
368 organosulfates in summertime Shanghai, China: potential influence of photochemical
369 processes and anthropogenic sulfate pollution, Atmos. Chem. Phys., 23, 13433-13450,
370 https://doi.org/10.5194/acp-23-13433-2023, 2023.
371 Yttri, K. E., Simpson, D., Nojgaard, J. K., Kristensen, K., Genberg, J., Stenström, K., Swietlicki,
372 E., Hillamo, R., Aurela, M., Bauer, H., Offenberg, J. H., Jaoui, M., Dye, C., Eckhardt, S.,
373 Burkhart, J. F., Stohl, A., and Glasius, M.: Source apportionment of the summer time
374 carbonaceous aerosol at Nordic rural background sites, Atmos. Chem. Phys., 11, 13339-13357,
375 https://doi.org/10.5194/acp-11-13339-2011, 2011.
376